A STUDY ON THE SHEAR STRENGTH EVALUATION METHOD
FOR MUD-PLASTERED WALLS

M. Nakao[1] and Y. Yamazaki[2]

ABSTRACT

This study was carried out to clarify the shear resisting mechanism and propose the shear strength evaluation method for mud-plastered walls. Firstly, shear loading tests of mud-plastered wall specimens with various types were completed. Secondly, the equations for evaluating the shear strength of mud-plastered walls were proposed based on simple macro models. The results showed a good agreement with the failure modes and shear strengths obtained from the shear loading tests for most specimens. Finally, structural analyses of the specimens by means of Rigid-Bodies-Spring Model were done. The analyzed shear strengths were close to the experimental values while the shear stiffness was higher than experimental ones.

Introduction

The mud-plastered wall is composed of a substrate woven of bamboos and some layers of mud mixed with straw and sand upon the substrate. Consequently, they are composed of completely natural materials.

These types of walls were commonly used as earthquake resisting elements in Japanese traditional houses. However, because of the collapse of a large number of wooden houses with mud-plastered walls during the recent earthquakes, such as the 1995 Hyogoken-Nanbu Earthquake, it was considered that their earthquake resistant performance was not good enough. Moreover, the seismic resistant performance of the mud-plastered walls in Japan has been under-evaluated by the design codes, mainly because of the lack of experimental data. Additionally, since the mud-plastered walls take a long period to be constructed, their manufacturing cost is higher than sheathed or bracing walls.

Mud-plastered walls have been rejected in the last 30 years for the above expressed reasons, but recently there is a move to recognize that they are suitable for the Japanese humid climate and also because they do not use chemicals, which can affect the health of the houses' residents.

This study is to clarify the shear resisting mechanism and to establish a shear strength evaluation method for mud-plastered walls by carrying out shear loading tests of mud-plastered walls with various types.

[1] Research Associate, Faculty of Engineering, Yokohama National University
[2] Professor, Faculty of Engineering, Yokohama National University

Construction of Mud-Plastered Wall

The mud-plastered wall is composed of a substrate woven of bamboos and some layers of mud mixed with straw and sand upon the substrate. The substrate consists of *Mawatashi* and *Komai*. *Mawatashi*s, which are bamboos of approximately 12 mm in diameter, are arranged as illustrated in Fig. 1(a). The ends of *Mawatashi*s are stuck in the holes of the wood frame. *Komai*s, which are chopped into pieces about 20 mm wide, are connected to the *Mawatashi*s by straw rope as shown in Photo 1. Fig. 1(b) shows the arrangement of *Mawarashi* and *Komai* from which some *Komai*s were omitted for simplicity in this illustration.
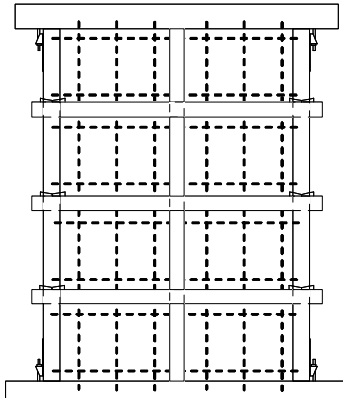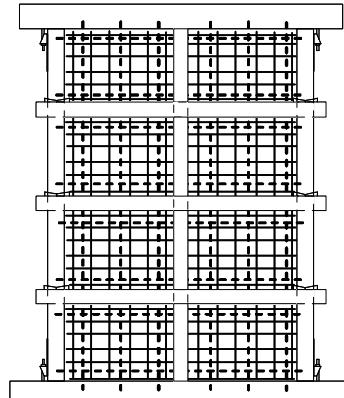
(a) Arrangement of *Mawatashi*s.   (b) Complete substrate.   Photo 1: Connecting *Komai*s to
Figure 1.   Arrangement of *Mawatashi*s and *Komai*s.   *Mawatashi*.
              (dashed line, *Mawatashi*; solid line, *Komai*)

The first and second layer of mud are called *Arakabe* and *Nakanuri* respectively. *Arakabe* is plastered with *Arakida*-clay that is produced in Tokyo surroundings and suitable for mud-plastered walls. In advance of plastering *Arakabe*, *Arakida*-clay is mixed with water and short cut rice straw. Approximately 3 months later, the clay has increased its viscosity by decomposition of the straw. This viscous mud is for *Arakabe*. The mud for *Nakanuri* is commonly obtained from *Arakabe*-mud mixed with additional water and sand. *Nakanuri* is plastered after the *Arakabe* is completely dried. At this time, a lot of cracks are observed on the surface of *Arakabe*, but no crack is observed on the surface of *Nakanuri* even after drying.
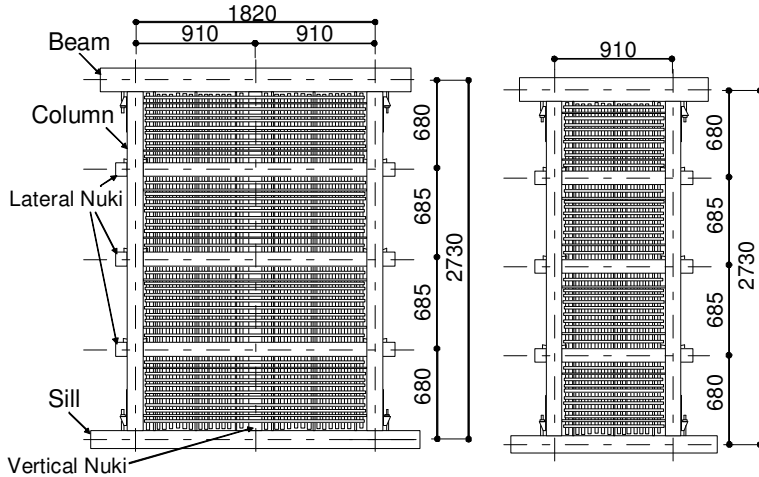
Outline of Experiment

Test Specimens of Mud-Plastered Walls

The test specimens were prepared as shown in Figs. 2, 3, 4 and Tables 1 and 2. The parameters were wall length, number of lateral *Nuki*s and thickness of the *Nakanuri*-layer. These factors are considered to influence the shear strength of mud-plastered walls.

To avoid the pulling-out of tenons from mortises, hold-down connectors (S-HD 15) were fastened to the end of columns by lag bolts and anchored to the horizontal members with anchor bolts.

The thickness of each layer of mud after they were completely dried is shown in Fig. 5.

(a) D-series specimen. (b) E-series specimen.

Figure 2. Scheme of specimens. (unit : mm)

Beam
Column
Lateral Nuki
Sill
Vertical Nuki

1820
910 910
680
685
685
680
2730

910
680
685
685
680
2730

Table 1. Specifications of members.

Member	Sizes(mm)	
Column	105x105	
Sill	105x135	Japanese cedar
Nuki	15x105	
Beam	105x180	Douglas fir

Table 2. List of specimens.

	Wall length (mm)	Thickness of plastered mud (mm)			Number of *Nuki*		Features
		Arakabe	*Nakanuri*		Lateral	Vertical	
			Lateral *Nuki* side	Vertical *Nuki* side			
D1	1820	30	0	0	3	1	*Arakabe* only
D2			15	15			Standard type
D2N			15	15	2		2 lateral *Nuki*s
D2T			25	25	3		Thick *Nakanuri*
D2L			15	0	3		One side *Nakanuri* only
D2V			0	15			One side *Nakanuri* only
E1	910	30	0	0	3	0	*Arakabe* only
E2			15	15			Standard type
E2N			15	15	4		4 lateral *Nuki*s
E2T			25	25	3		Thick *Nakanuri*
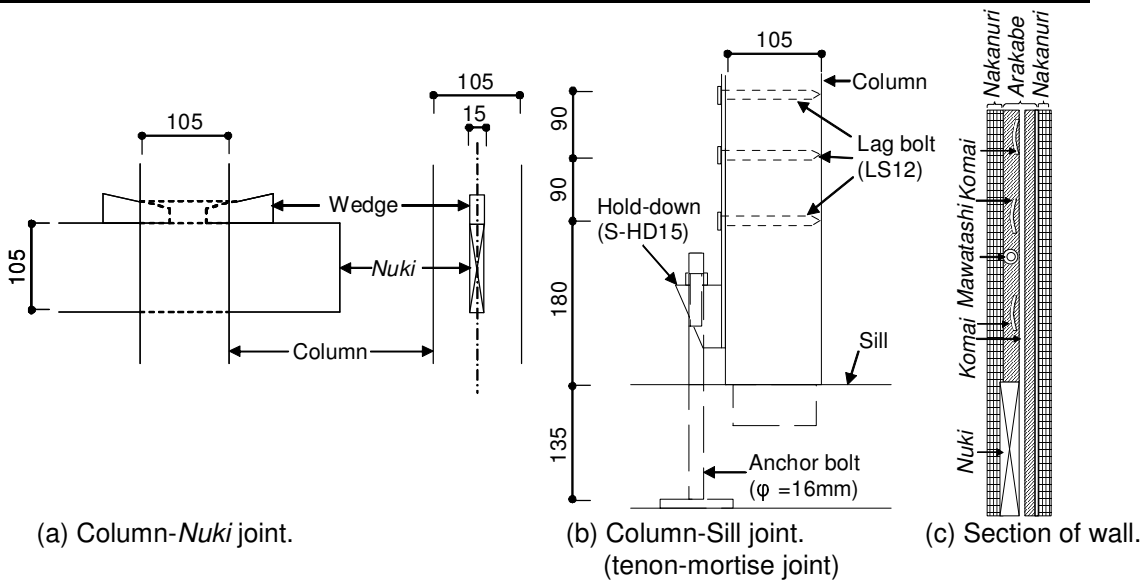
(a) Column-*Nuki* joint. (b) Column-Sill joint. (tenon-mortise joint) (c) Section of wall.

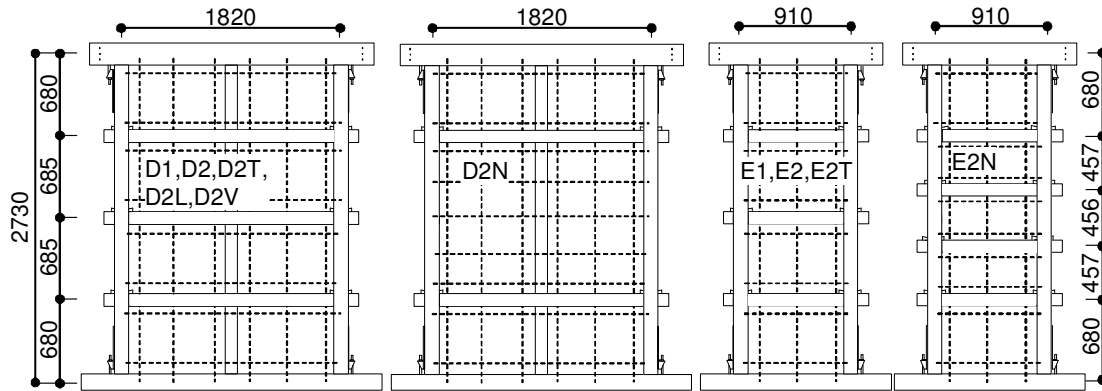Figure 3. Details of specimens (mm).

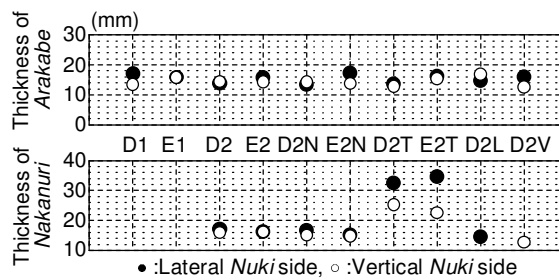Figure 4. Arrangement of *Mawatashi*s (mm).

Figure 5. Thickness of *Arakabe* and *Nakanuri.*

Loading and Measuring Procedure

The wall specimen was fastened to the test apparatus beam at the sill, as shown in Fig. 6, and torsion stopping rollers were applied along the beam of the specimen. Lateral static load was applied to the beam of the wall specimen following the static cyclic history shown in Fig. 7, while no vertical load was applied. Before starting the test, to prevent the hold-downs being subjected to tensile forces, the anchor bolts nuts were loosened, but left still touching the hold-downs. In addition, transducers were set to measure the deformation of the wood frame as shown in Fig. 8.
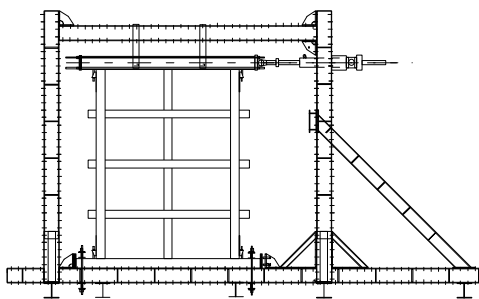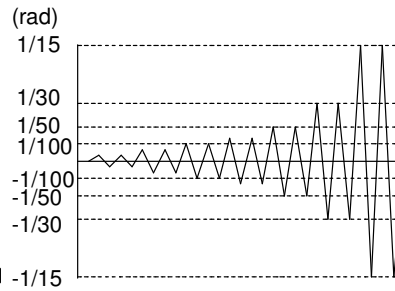

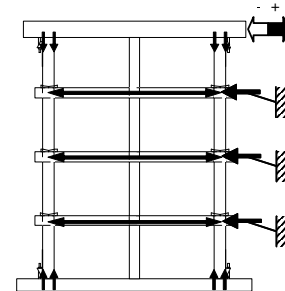Figure 6. Setup of shear loading test.   Figure 7. Cyclic history.   Figure 8. Measured portions.

Test Results

Failure Mode and Hysteresis Characteristic of Wall Specimen

Fig. 9 shows the relation between the drift angle based on horizontal displacement at the beam and the shear force. In *Arakabe* specimens, such as D1 and E1, the shear forces increased gradually until the ends of the tests, but showing low shear stiffness. Comparing with frame specimens (Nakao and

Yamazaki 2004), a small amount of shear forces are carried by the *Arakabe*-layer itself.

In *Nakanuri* specimens with 1820mm of wall length, while in the small deformation level, corners of the *Nakanuri*-layer along sill and beam crushed and the *Nakanuri*–layer with the *Arakabe*–layer rotated together with an increase in the shear deformation of the wood frame. At 1/150rad of drift angle, in *Nakanuri* specimens except for D2T, shear cracks occurred. It was at 1/75rad that the shear crack was observed in D2T. The maximum shear force was provided at 1/100 rad in D2L and D2V while in the other specimens at 1/50 rad. Crack patterns when the maximum shear force was attained are shown in Fig. 10. In D2, D2N, D2L and D2V, shear slip failure was observed along lateral *Nuki*s. However, such failure mode was not seen in D2T. Moreover, since the crush of corners of the *Nakanuri*–layer along the end of column occurred in every *Nakanuri* specimen, it is considered that the shear force applied to the specimen is transferred from the top end of column to the *Nakanuri*-layer.

In *Nakanuri* specimens with 910mm of wall length, such as E2, E2N and E2T, the crush of corners of the *Nakanuri*–layer along sill and beam was remarkable. The rotation angle of the *Nakanuri*-layer was larger than the one of the specimen with 1820mm of wall length. About 1/50 rad of drift angle, the *Nakanuri*–layer at the corners and around the joints of columns and *Nuki*s swelled out of plane. The crack along the lateral *Nuki* in E2 and E2N occurred due to the swelling out of *Nakanuri*-layer. Such a failure mode observed in these specimens, E2, E2N and E2T, is defined as "*Nakanuri*–rocking" failure. In the specimens with 910mm of wall length, shear crack was observed only in E2N at 1/30 rad.

In this experiment, the failure modes of mud-plastered wall specimens were classified into two types, namely, shear slip failure and *Nakanuri*-rocking failure. Fig. 11 shows the two failure modes of mud-plastered walls. The failure mode of *Nakanuri* specimens with 1820mm of wall length except for D2T was shear slip failure, while the one of the other specimens was *Nakanuri*-rocking failure. Considering the crack pattern, the failure mode of D2T is considered to be *Nakanuri*-rocking failure.
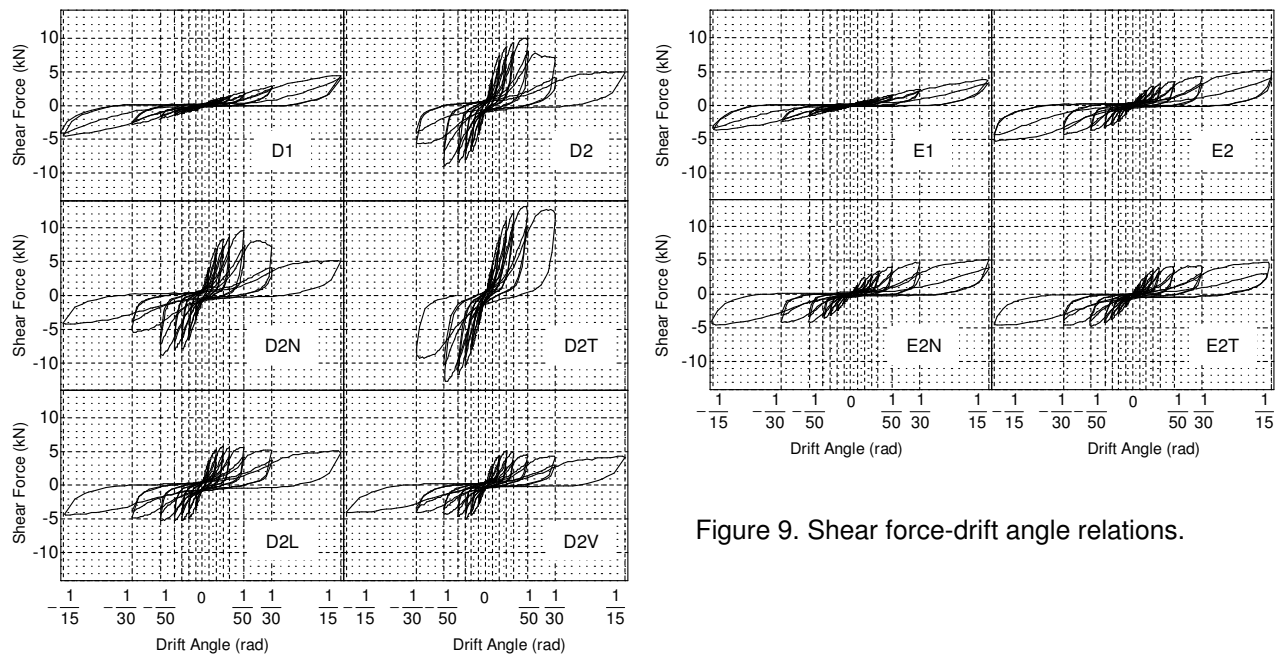

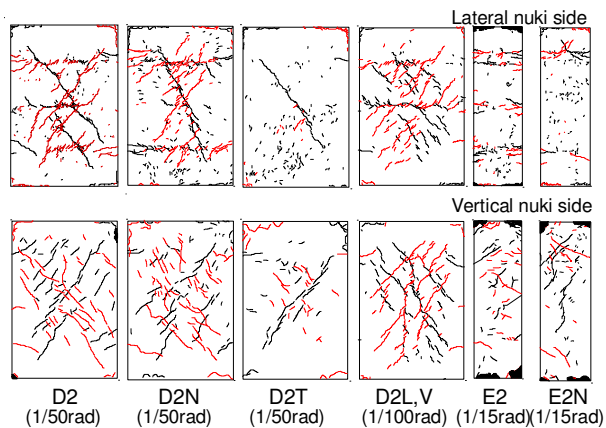Figure 9. Shear force-drift angle relations.
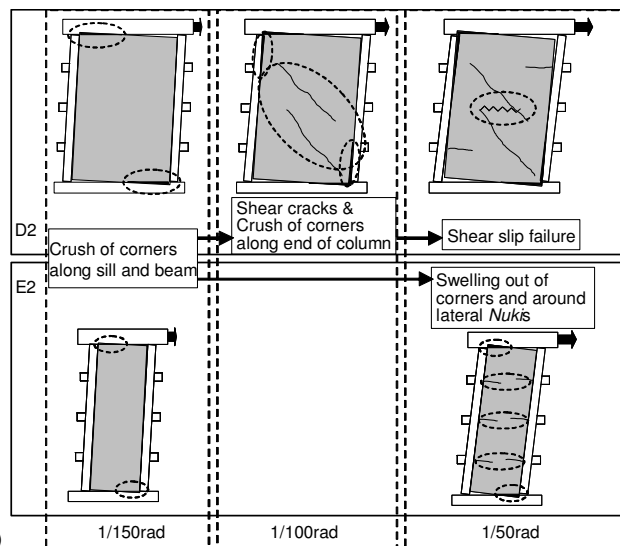
Figure 10. Crack patterns.

Figure 11. Difference between two failure modes.

Material Characteristics of Mud

Uniaxial compression and tension tests were conducted to evaluate the material characteristics of mud during the same period as the shear loading tests of the walls specimens. The dimension of the test piece was 50mm in diameter and 100mm in height. Five test pieces were prepared for each mud and for compression and tension tests respectively.

Some of the typical test results are shown in Fig. 12. The compressive stress of *Arakabe*-mud increased gradually as the displacement increased. *Nakanuri*-mud reached maximum stress with approximately 2mm of displacement, failing down rapidly after that point.

In addition, the average compressive strength of *Arakabe*-mud is 0.31N/mm^2, while for *Nakanuri*-mud the value is 0.54N/mm^2. On the other hand, the tensile strength is 0.05N/mm^2 in *Arakabe*-mud and 0.10N/mm^2 for *Nakanuri*–mud.
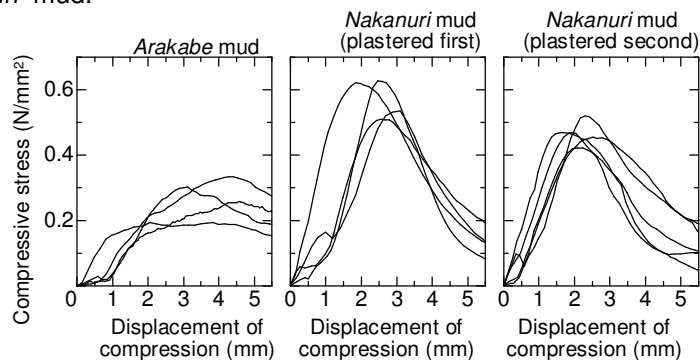

Figure 12. Stress-displacement relationship of mud.

Proposed Shear Strength Evaluation Method

Equations for evaluating the shear strength

From the experimental results, equations for evaluating the shear strength of mud-plastered walls are proposed as follows. In these equations, the *Arakabe*-layer is neglected while the *Nakanuri*-layer is considered because a small amount of shear force is carried by the *Arakabe*-layer.

In case the failure mode is shear slip failure, the shear cracks appear first and the shear slip failure occurs when the maximum shear force is provided. Therefore, considering the shear resisting model as shown in Fig. 13(a), the shear strength when the shear slip failure occurs (V_s) is expressed by Eq. 1.

$$V_s = {}_n\sigma_c \cdot t_n \cdot l_w / 4 \tag{1}$$

where ${}_n\sigma_c$ is compressive strength of *Nakanuri*-mud, t_n is thickness of the *Nakanuri*–layer and l_w is the inside measurement between both columns.

In case the failure mode is *Nakanuri*-rocking failure, the shear resisting model is shown as Fig. 13(b). Therefore, the shear strength when the *Nakanuri*-rocking failure occurs (V_{co}) is expressed by Eqs 2-5.

$$V_{co} = {}_cV_{co} + {}_nV_{co} + {}_mV_{co} \tag{2}$$
$$ {}_cV_{co} = 0.167 \cdot {}_n\sigma_c \cdot t_n \cdot l_w 2 / H \tag{3}$$
$$ {}_nV_{co} = 0.167 \cdot {}_n\sigma_c \cdot t_b \cdot l_w 2 \cdot n_L / H \tag{4}$$
$$ {}_mV_{co} = p_m \cdot n_m \cdot l_w / H \tag{5}$$

where ${}_cV_{co}$ is the shear force contributing to the crush of the corner of the *Nakanuri*-layer, ${}_nV_{co}$ is the shear force contributing to the crush around lateral *Nuki*, ${}_mV_{co}$ is the shear force contributing to the crush around *Mawatashi*, 0.167 is a coefficient in the case of a triangular stress distribution, t_b is the thickness of lateral *Nuki*, n_L is the number of lateral *Nuki*, p_m is the dowel shear resisting force of *Mawatashi* due to the gap between the wood frame and the *Nakanuri*-layer, n_m is number of lateral *Mawatshi* and H is the height of loading.

(a) In case shear slip mode.　　　　　　　　　　(b) In case mud-rocking failure mode.
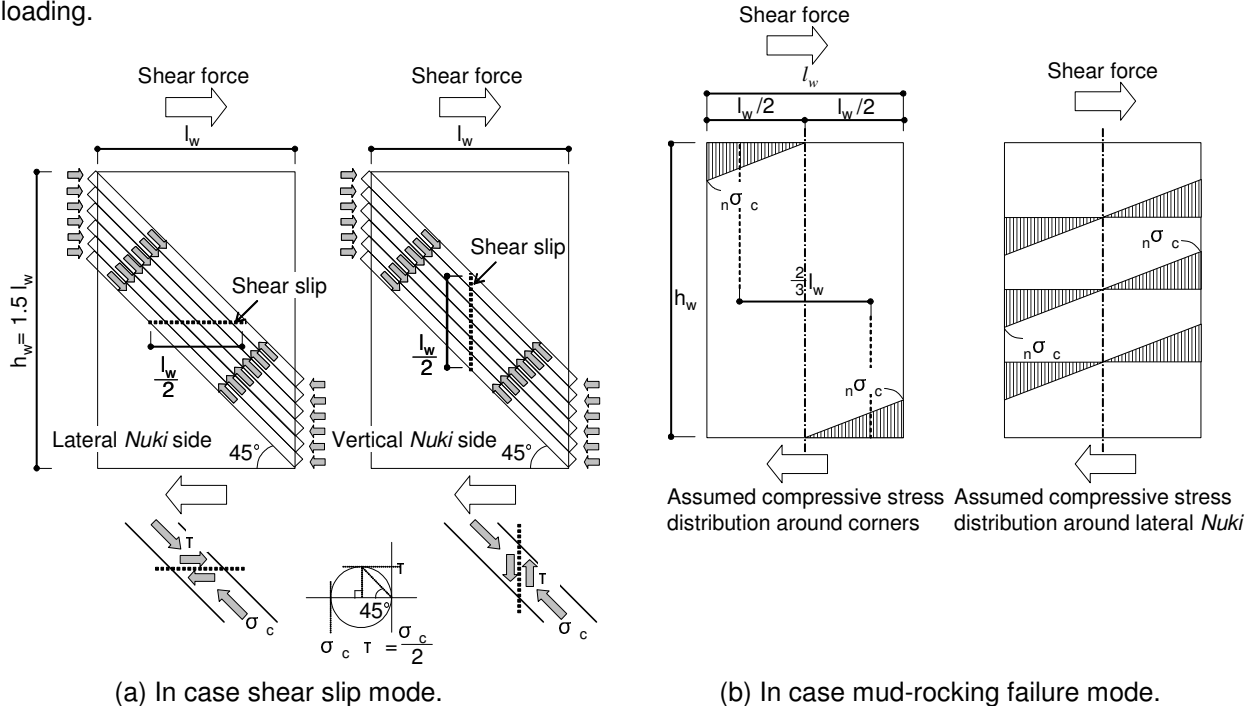
Figure 13. Shear resisting models.

Comparison between calculated and experimental values

Table 3 shows the calculated shear strengths by means of proposed equations and experimental results. The experimental shear strength, V_{exp}, is the shear force carried by the *Nakanuri*–layer that is calculated by subtracting the shear force of the *Arakabe* specimen from the *Nakanuri* specimen. To calculate the shear strengths, the average values in compression tests of mud, $_n\sigma_c = 0.54$ N/mm^2, was used. In addition, p_m is assumed to be 0.2kN.

The calculated shear strengths corresponding to the observed failure modes in the experiments are close to the experimental shear strengths in D2, D2N, D2T, E2, E2N and E2T. However, the calculated values of D2L and D2V are about 20% lower than the experimental values. Moreover, considering that the failure mode corresponding to the minimum value of the two shear strengths, namely V_{co} and V_s, gives the calculated failure mode, good correspondence is observed for most of specimens.

The differences between the calculated and experimental values are due to some assumptions in the equations. These equations are based on limited experimental data. For improving the precision of the proposed equations, more experimental data with various mud-plastered walls are needed.

Table 3. Calculated and experimental shear strengths. (unit : kN)

	D2	D2N	D2T	D2L	D2V	E2	E2N	E2T
Failure mode in experiment	Shear slip		Rocking	Shear slip		Rocking		
$_cV_{co}$	3.21	3.11	5.64	1.46	1.26	0.68	0.64	1.22
$_nV_{co}$	4.37	2.91	4.37	4.37	4.37	0.96	1.28	0.96
$_mV_{co}$	1.01	1.13	1.01	1.01	1.01	0.47	0.59	0.47
V_{co} $(=_cV_{co}+_nV_{co}+_mV_{co})$	8.58	7.15	<u>11.01</u>	6.83	6.64	<u>2.12</u>	<u>2.52</u>	<u>2.66</u>
V_s	<u>7.64</u>	<u>7.41</u>	13.43	<u>3.47</u>	<u>3.01</u>	3.48	3.26	6.19
V_{exp}	7.78	7.60	10.96	4.38	3.98	2.05	2.53	2.78

underline : calculated shear strength corresponding to experimental failure mode

RBSM Analysis

Analytical Method

As shown above, the shear strengths of mud-plastered walls were able to be calculated by means of the proposed equations for most specimens. For obtaining more information regarding the seismic performance of mud-plastered walls, structural analysis must to be conducted. In the Rigid Bodies Spring Model (RBSM) (Kawai 1977), it is assumed that elements are rigid and that the spring connecting two elements to each other has material characteristics. Therefore, simulating failure modes, such as shear crack, shear slip and crush of the *Nakanuri*-layer, is relatively easy.

The analysis model of the mud-plastered wall specimen with 1820mm of wall length is shown in Fig. 14. The wood frame is assumed to be elastic and consists of squared elements, while the shape of the *Nakanuri* element is a hexagon. The elastic modulus of Japanese cedar (column, sill and *Nuki*) and Douglas fir (beam) are assumed to be 7kN/mm^2 and 12kN/mm^2 respectively.

The stress-strain curve and shear slip model for *Nakanuri*-mud in this analysis are assumed as Fig. 15. For compressive and tensile strength, the average values in compression and tension tests of *Nakanuri*-mud were used. The *Arakabe*-layer is not considered in this analysis model.

Lateral *Nuki* elements are connected to both sides of the columns by pin joint and *Nakanuri* elements. There are link elements between the *Nuki* elements and *Nakanuri* elements as shown in Fig. 16. The stress-relative displacement relationship of link elements is perfectly elastic-plastic, and the yield stress and displacement are 0.54N/mm^2 and 3mm respectively. The dowel shear stiffness and yield shear force of *Mawatashi* are assumed to be approximately 0.07kN/mm and 0.2kN per one portion respectively.

As the *Nakanuri*-layer does not stick to the wood frame, boundary elements were set between the *Nakanuri* elements and wood frame elements as shown in Fig. 17. The tensile and shear strength of the boundary element were assumed to be 0.01 times of the values of *Nakanuri*-mud while the elastic modulus and compressive strength were equal to the ones of *Nakanuri*-mud. Static incremental load was applied to the end of the beam until the lateral stiffness had disappeared.
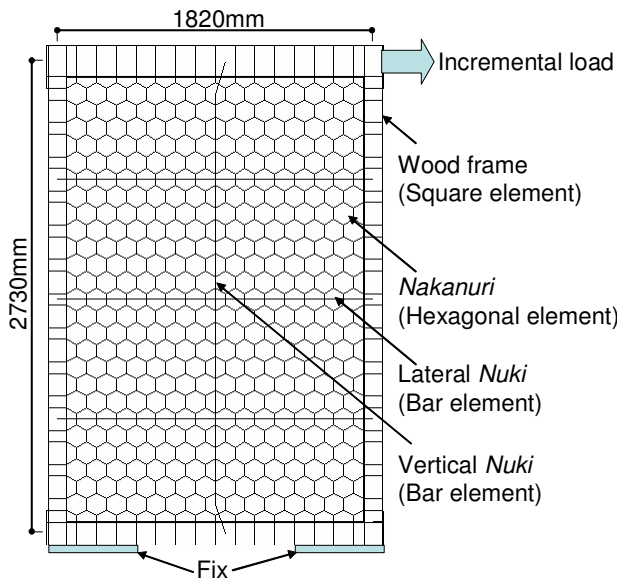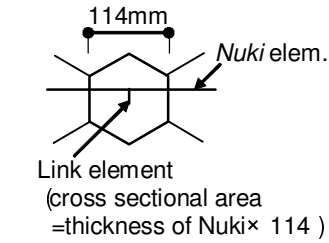
Figure 14. Analysis model.
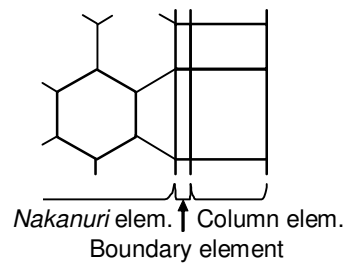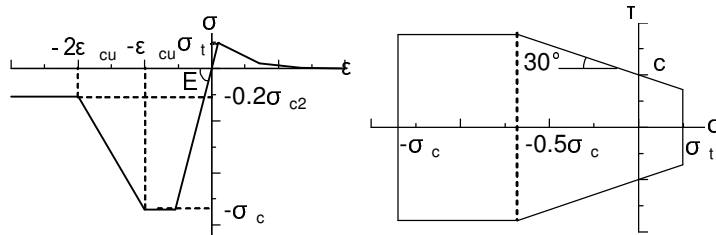
Figure 16. Link element.

Figure 17. Boundary element.

Poisson's coefficient ν	Elastic modulus E(N/mm^2)	Yeild stress σ_c(N/mm^2)
0.167	200	0.54
Tensile strength σ_t(N/mm^2)	Shear strength c(N/mm^2)	Limit compressive strain ε_{cu}
0.098	0.2	0.005

Figure 15. Stress-strain curve and shear slip model of *Nakanuri*-mud.

Comparison Between Analyzed and Experimental Results

Fig. 18 shows the analyzed results and the skeleton curves of the experimental results. In this figure, the vertical axes are shear force carried by *Nakanuri*. The analyzed results are shown only up to near the point of maximum strength because the lateral stiffness of the analysis model became almost zero and could not resist the additional incremental load.

The initial stiffness of analysis is higher than the experimental one while the analyzed maximum shear force carried by the *Nakanuri*–layer is close to the experimental value in most specimens.

The assumptions, such as the elastic modulus of *Nakanuri*-mud, the yield stress of link element and the dowel shear stiffness of *Mawatashi*, have much influence on the shear stiffness and strength of mud-plastered walls. Therefore, inspecting the values by means of experiments are needed.
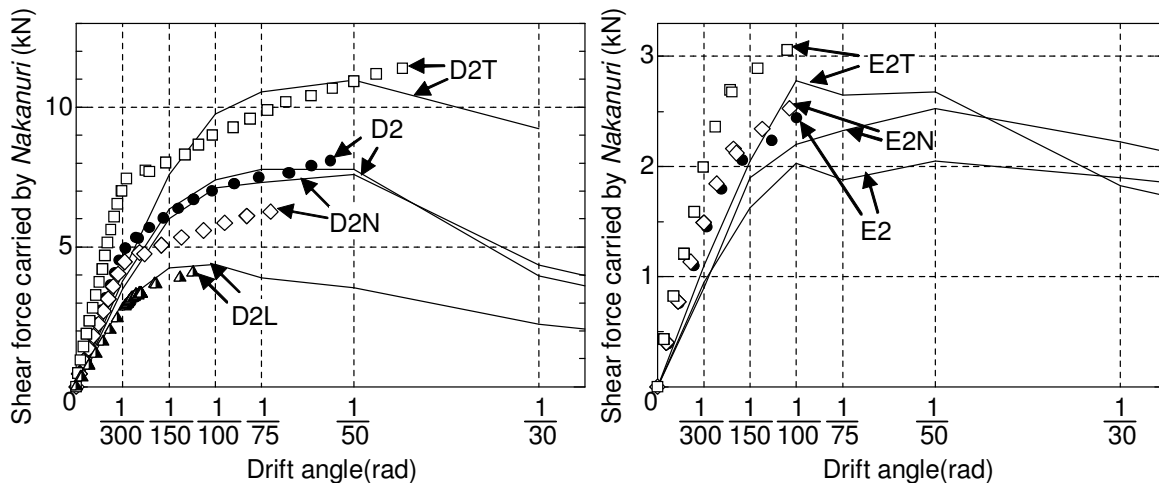
Figure 18. Analyzed and experimental result. (Lines : experiment, dots : analysis)

Conclusions

To clarify the shear resisting mechanism and propose the shear strength evaluation method for mud-plastered walls, shear loading tests of mud-plastered wall specimens with various types were made. From the experimental results, the equations for evaluating the shear strength of mud-plastered walls were proposed. The equations provided close values to the experimental shear strengths for most specimens, however, there were underestimations for some specimens. Moreover, the analyses of the specimens by means of Rigid-Bodies-Spring Model were completed. The analyzed shear strengths were close to experimental values while the shear stiffness was higher than experimental ones. Since the proposed equations and the analysis model are based on limited experimental data, they contain many assumptions. For improving the precision of the proposed equations and analysis model, more experimental data with various mud-plastered walls are needed.

References

Nakao, M., and Yamazaki, Y., 2004. Experimental Study on the Evaluation of the Earthquake Resistant Performance of Mud-plastered Walls, 13th world Conference on Earthquake Engineering, No. 1878

Kawai, T., 1977. New Element Models in Discrete Structural Analysis, Journal of the Japan Society of Naval Architects and Ocean Engineers, 174-180